

Syntheses and Crystal Structures of Ruthenium and Rhodium Olefin Complexes Containing GaCp*[†]

Thomas Cadenbach, Christian Gemel, Timo Bollermann, and Roland A. Fischer*

Anorganische Chemie II - Organometallics & Materials, Ruhr-Universität Bochum, D-44780 Bochum, Germany

Received November 28, 2008

The reactivity of olefin containing complexes of the d⁸ metals Ru⁰ and Rh^I toward GaCp* and AlCp* is presented. [Ru(η^4 -butadiene)(PPh₃)₃] reacts with GaCp* to give the substitution product [Ru(η^4 -butadiene)(PPh₃)₂(GaCp*)] (**1**), which proved to be stable in the presence of GaCp* even under hydrogenolytic conditions. In contrast, the bis-styrene complex [Ru(PPh₃)₂(styrene)₂] undergoes full substitution of the olefin ligands to give [Ru(PPh₃)₂(GaCp*)₃] (**2**), whereas reaction of [Ru(η^2, η^2 -COD)(η^6 -COT)] (COD = 1,5-cyclooctadiene, C₈H₁₂, COT = 1,3,5-cyclooctatriene, C₈H₁₀) and GaCp* leads to [Ru(η^2, η^2 -COD)(GaCp*)₃] (**3**) under mild hydrogenolytic conditions. Analogously, the Rh^I compounds [[Rh(η^2, η^2 -NBD)(PCy₃)₂]{BAR^F}] (NBD = norbornadiene) and [[Rh(η^2, η^2 -COD)₂]{BAR^F}] (BAR^F = B{[C₆H₃(CF₃)₂]₄}) yield the complexes [[Rh(η^2, η^2 -NBD)(PCy₃)(GaCp*)₂]{BAR^F}] (**4**), [[Rh(η^2, η^2 -COD)(GaCp*)₃]{BAR^F}] (**5**), and [[Rh(η^2, η^2 -COD)(AlCp*)₃]{BAR^F}] (**6**) upon reaction with the appropriate ECp* ligand (E = Al, Ga). All new complexes have been characterized by means of ¹H and ¹³C NMR spectroscopy and elemental analysis, as well as X-ray single crystal structure analysis in the case of **1–5**.

Introduction

The chemistry of low valent group 13 organyls E^IR (E = Al, Ga, In; R = alkyl, aryl, Cp*, amides, β -diketiminate, amidinates, guanidinates) with respect to their coordination properties to transition metal centers is a growing new field in inorganic coordination chemistry.^{1–14} The unique bonding situation of the metal–metal bonds present in such

compounds has been pointed out in numerous publications, including a number of reviews and highlights, particularly emphasizing the remarkable σ -donor properties of ER, together with the high electrostatic character of the resulting M–E bond.¹⁵ Only recently, few groups have started to investigate the organometallic chemistry of complexes of general formula [L_nM_d(ER)_b]. In this context, the Cp* substituent is particularly interesting because of its soft binding properties and its use as a flexible protection group for the group-13 center, in particular for Ga.^{16–22} The formation of the remarkable zinc coordination/cluster compounds [Mo(ZnMe)₉(ZnCp*)₄] and [Mo(CO)₄]₄(Zn)₆(μ -ZnCp*)₄] serves as an especially illustrative example.^{23,24}

[†] Organo group 13 complexes of transition metals LVIII; communication LVIII see ref 32.

*To whom correspondence should be addressed. E-mail: roland.fischer@ruhr-uni-bochum.de. Fax: (+49)234 321 4174.

- (1) Jones, C.; Junk, P. C.; Platts, J. A.; Stasch, A. *J. Am. Chem. Soc.* **2006**, *128*, 2206–2207.
- (2) Baker, R. J.; Jones, C. *Coord. Chem. Rev.* **2005**, *249*, 1857–1869.
- (3) Minasian, S. G.; Krinsky, J. L.; Williams, V. A.; Arnold, J. *J. Am. Chem. Soc.* **2008**, *130*, 10086–10087.
- (4) Linti, G.; Schnoekel, H. *Coord. Chem. Rev.* **2000**, *206–207*, 285–319.
- (5) Gemel, C.; Steinke, T.; Cokoja, M.; Kempter, A.; Fischer, R. A. *Eur. J. Inorg. Chem.* **2004**, 4161–4176.
- (6) Fischer, R. A.; Weiss, J. *Angew. Chem., Int. Ed.* **1999**, *38*, 2831–2850.
- (7) Hardman, N. J.; Eichler, B. E.; Power, P. P. *Chem. Commun.* **2000**, 1991–1992.
- (8) Hardman, N. J.; Wright, R. J.; Phillips, A. D.; Power, P. P. *J. Am. Chem. Soc.* **2003**, *125*, 2667–2679.
- (9) Baker, R. J.; Farley, R. D.; Jones, C.; Kloth, M.; Murphy, D. M. *Dalton Trans.* **2002**, 3844–3850.
- (10) Kuchta, M. C.; Bonanno, J. B.; Parkin, G. *J. Am. Chem. Soc.* **1996**, *118*, 10914–10915.
- (11) Schmidt, E. S.; Jockisch, A.; Schmidbaur, H. *J. Am. Chem. Soc.* **1999**, *121*, 9758–9759.
- (12) Dohmeier, C.; Loos, D.; Schnoekel, H. *Angew. Chem., Int. Ed. Engl.* **1996**, *35*, 129–149.
- (13) Uhl, W.; Pohlmann, M.; Wartchow, R. *Angew. Chem., Int. Ed.* **1998**, *37*, 961–963.
- (14) Seifert, A.; Linti, G. *Inorg. Chem.* **2008**, *47*, 11398–11404.

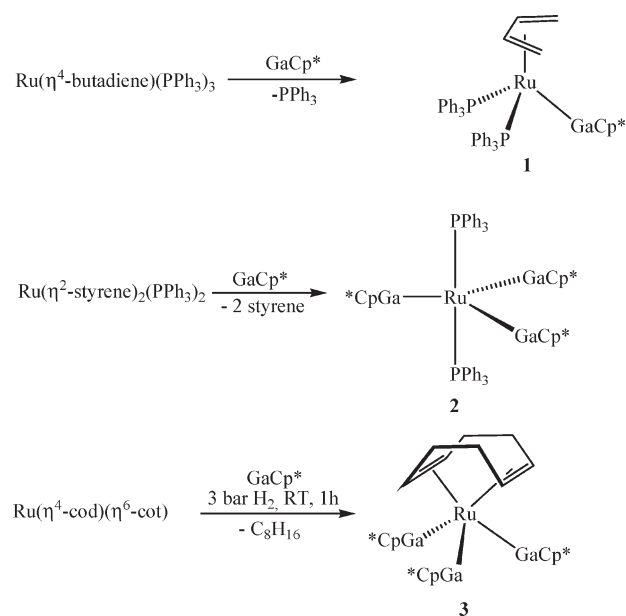
- (15) Frenking, G.; Froehlich, N. *Chem. Rev.* **2000**, *100*, 717–774.
- (16) Cadenbach, T.; Gemel, C.; Schmid, R.; Fischer, R. A. *J. Am. Chem. Soc.* **2005**, *127*, 17068–17078.
- (17) Cadenbach, T.; Gemel, C.; Zacher, D.; Fischer, R. A. *Angew. Chem., Int. Ed.* **2008**, *47*, 3438–3441.
- (18) Steinke, T.; Gemel, C.; Winter, M.; Fischer, R. A. *Chem.—Eur. J.* **2005**, *11*, 1636–1646.
- (19) Steinke, T.; Gemel, C.; Cokoja, M.; Winter, M.; Fischer, R. A. *Angew. Chem., Int. Ed.* **2004**, *43*, 2299–2302.
- (20) Steinke, T.; Cokoja, M.; Gemel, C.; Kempter, A.; Krapp, A.; Frenking, G.; Zenneck, U.; Fischer, R. A. *Angew. Chem., Int. Ed.* **2005**, *44*, 2943–2946.
- (21) Jutzi, P.; Neumann, B.; Schebaum, L. O.; Stammer, A.; Stammer, H.-G. *Organometallics* **1999**, *18*, 4462–4464.
- (22) T. Cadenbach, T. Bollermann, C. Gemel, R. A. Fischer, *Dalton Trans.* [Online early access]. DOI: . Published Online: 2009; in press.
- (23) Cadenbach, T.; Gemel, C.; Fischer Roland, A. *Angew. Chem., Int. Ed.* **2008**, *47*, 9146–9149.
- (24) Cadenbach, T.; Bollermann, T.; Gemel, C.; Fernandez, I.; von Hopfgarten, M.; Frenking, G.; Fischer Roland, A. *Angew. Chem., Int. Ed.* **2008**, *47*, 9150–9154.

Although ER ligands are formally described in terms of their isolobal analogy to CO, their coordination properties are in fact rather different and also depend on the R substituents to a large extent. For instance, homoleptic clusters $[M_a(ECp^*)_b]$ ($a = 2-6$) are known for the d^{10} metals Ni, Pd, and Pt; however, their molecular structures are in all cases different from those of the corresponding homoleptic carbonyl clusters.¹⁸ Since the direct substitution of CO by ECp^* is generally limited because of the increasing π -backbonding character of the metal centers on introduction of the ligands, the usual route for the synthesis of $[M_a(ECp^*)_b]$ involves substitution of more labile olefin ligands.^{18,20,21} So far, only the use of sterically encumbering Ga^I ligands $Ga(DDP)$ ²⁵ ($DDP = 2\text{-}\{(2,6\text{-diisopropylphenyl})\text{amino}\}\text{-4}\text{-}\{(2,6\text{-diisopropylphenyl})\text{imino}\}\text{-2-pentene}$) or $[Ga\{N(Ar)\text{-}C(H)_2\}]^-$ ²⁵ ($Ar = C_6H_3^t Pr_2\text{-}2,6$) has permitted Ga^I transition metal complexes containing olefins as co-ligands to be isolated, whereas in the case of ECp^* , full substitution of the olefin ligands has always been observed. However, the very unusual structure of the Ni_3 cluster $[\{\mu^2 Ga(DDP)\}Ni(\text{ethylene})_2Ni(\mu^2 CH=CH_2)(H)]$ formed by C–H activation of ethylene and featuring a vinyl ligand bridging all three nickel centers, suggests that the most structurally interesting varieties of Ga^I clusters could be obtained in the presence of olefin ligands.²⁶ Thus, it seemed promising to us to study also the coordination of ECp^* ($E = Al, Ga$) to metal centers binding olefin co-ligands. The control of the M/E ratio in the obtained compounds is also important, as they might be used as precursors for subsequent transformations, similarly to the synthesis of the above-mentioned compounds such as $[Mo(ZnMe)_9(ZnCp^*)_3]$.²⁴ In this paper we present the reaction of ECp^* with the d^8 transition metal centers Ru^0 and Rh^I known to be generally rather basic, thus binding olefins quite strongly, which would inhibit full substitution of the olefin ligands.

Results and Discussion

Reaction of the ruthenium complex $[Ru(\eta^4\text{-}1,3\text{-butadiene})(PPh_3)_3]$ with one molar equivalent of $GaCp^*$ in toluene results in substitution of one triphenylphosphine ligand by $GaCp^*$ and formation of $[Ru(\eta^4\text{-}1,3\text{-butadiene})(PPh_3)_2(GaCp^*)]$ (**1**) (see Scheme 1). The ¹H NMR of **1** shows the expected singlet signal for the $GaCp^*$ ligand at $\delta = 1.82$ ppm and in addition a set of signals for the butadiene ligand at $\delta = 4.81$ (br, 2H, syn 1,4-CH₂), 2.52 (br, 2H, CH), and -0.54 (br, 2H, anti 1,4-CH₂) ppm, pointing to a rotation of the butadiene ligand around the metal ligand bond on the NMR time scale, which is well consistent with the generally high fluxionality for 5-fold coordinated d^8 centers. The ³¹P NMR reveals one singlet at 66.1 ppm. Single crystals suitable for X-ray diffraction studies were obtained by slowly cooling a saturated toluene solution of **1** down to -30 °C for several days. Important crystallographic data are summarized in Table 1, and the molecular structure is shown in Figure 1. Compound **1** crystallizes in the triclinic space group $P\bar{1}$. The complex adopts a strongly distorted trigonal-bipyramidal structure with one phosphine ligand (P(2)) and one double bond of the diolefin ligand (C(1)C(2)) in the axial positions and the second double bond of the butadiene ligand (C(3)C(4)) as well as the remaining triphenylphosphine ligand (P(1)) and the $GaCp^*$ ligand in the equatorial positions. The axial part of the butadiene ligand is found to be rather strongly bent

Scheme 1. Synthesis of the Ruthenium Complexes **1**, **2**, and **3**



toward the equatorial plane resulting in angles $C(1)C(2)_{Cent.}-Ru-P(2)$ of 137.2° and $P(1)-Ru-C(1)C(2)_{Cent.}$ of 118.4° . The angles between the equatorial ligands sum up to 355.2° , which is consistent with the proposed trigonal-bipyramidal structure. The $Ru-GaCp^*$ bond length of 2.401 (1) Å is comparable to other $Ru-Ga$ complexes, and the Cp^* group is η^5 -bound to the Ga atoms with a $Ga-Cp^*_{centr.}$ bond length of 2.001 Å.^{22,27,28} The $Ru-P$ bond lengths average to 2.304 Å which is within the range for $Ru-P$ bond lengths reported in the literature. The butadiene ligand is bound in a typical η^4 binding mode with $Ru-C$ distances ranging from $Ru-C(3)$ $2.154(4)$ Å to $Ru-C(1)$ $2.202(4)$ Å, with an average distance of 2.179 Å. The $C(1)-C(2)$ and the $C(3)-C(4)$ distances are $1.430(6)$ and $1.423(5)$ Å, whereas the $C(2)-C(3)$ Å distance ($1.396(5)$ Å) is distinctly shorter. This points to a metallacyclopentene structure rather than a simple π -complex and thus to a high degree of π -backbonding.²⁹⁻³¹

Treatment of **1** with excess of $GaCp^*$ under an atmosphere of hydrogen in toluene at 110 °C does not lead to further substitution of the phosphine ligands or hydrogenation of the butadiene. However, reaction of the 16 electron ruthenium complex $[Ru(\text{styrene})_2(PPh_3)_2]$ with 3 molar equiv of $GaCp^*$ leads to a full substitution of the olefin ligands and formation of $[Ru(PPh_3)_2(GaCp^*)_3]$ (**2**) (Scheme 1). The ¹H NMR spectrum of **2** in C_6D_6 at room temperature shows a multiplet signal at $\delta = 8.06-7.00$ ppm for the PPh_3 ligands and one singlet signal at $\delta = 1.67$ ppm, which can be assigned to the $GaCp^*$ ligands. By slowly cooling a saturated solution of **2** in n -hexane to -30 °C, red crystalline needles can be isolated in good yields. The molecular structure of **2** consists of a trigonally bipyramidally coordinated ruthenium center, with the PPh_3 ligands in the equatorial and the $GaCp^*$ ligands in the axial positions. It should be noted, that the crystals lose their monocrystallinity after more than 12 h even at low temperatures (100 K), and therefore the data quality of the X-ray analysis is rather poor but still sufficiently accurate to confirm the connectivity of the atoms in the molecule. A POVray plot of **2** is shown in the Supporting Information.

Table 1. Important Crystallographic Data of Compounds 1 and 3–6^a

	1	3	4	5	6
empirical formula	C ₅₀ H ₅₁ GaP ₂ Ru	C ₃₈ H ₅₇ Ga ₃ Ru	C ₇₇ H ₈₃ BF ₂₄ Ga ₂ PRh	C ₇₀ H ₆₉ BF ₂₄ Ga ₃ Rh	C ₇₀ H ₆₉ Al ₃ BF ₂₄ Rh
molecular weight	884.64	824.07	1748.56	1689.13	1560.91
temperature (K)	100(2)	113(2)	100(2)	106(2)	105(2)
wavelength Mo-K α (Å)	0.71073	0.71073	0.71073	0.71073	0.71073
crystal size (mm)	0.15 × 0.1 × 0.1	0.25 × 0.15 × 0.1	0.2 × 0.15 × 0.1	0.2 × 0.15 × 0.10	0.30 × 0.20 × 0.15
crystal system, space group	triclinic, <i>P</i> $\bar{1}$	triclinic, <i>P</i> $\bar{1}$	monoclinic, <i>P</i> 2(1)/ <i>n</i>	orthorhombic, <i>Pna</i> 2(1)	orthorhombic, <i>Pna</i> 2(1)
<i>a</i> (Å)	11.345(3)	10.693(4)	15.8148(4)	24.941(7)	25.022(6)
<i>b</i> (Å)	13.493(3)	11.111(4)	25.0768(9)	19.361(6)	19.373(5)
<i>c</i> (Å)	14.575(4)	17.202(6)	19.0581(8)	14.669(5)	14.526(5)
α (deg)	89.35(2)	81.52(3)	90	90	90
β (deg)	68.43(2)	76.88(3)	92.723(3)	90	90
γ (deg)	83.562(19)	67.23(3)	90	90	90
cell volume (Å ³)	2060.7(9)	1831.3(11)	7549.6(5)	7083(4)	7042(3)
<i>Z</i>	2	2	4	4	4
density ρ_{calc} . (g cm ⁻³)	1.426	1.494	1.538	1.584	1.472
absorption coefficient μ (mm ⁻¹)	1.132	2.612	1.048	1.461	0.384
<i>F</i> (000)	912	844	3552	3392	3176
θ range for data collection (deg)	3.04–27.56	3.39–36.86	3.31–27.68	3.01–25.05	3.01–25.06
index ranges	−14 ≤ <i>h</i> ≤ 14, −17 ≤ <i>k</i> ≤ 17, −16 ≤ <i>l</i> ≤ 18	−17 ≤ <i>h</i> ≤ 15, −13 ≤ <i>k</i> ≤ 16, −27 ≤ <i>l</i> ≤ 24	−20 ≤ <i>h</i> ≤ 20, −32 ≤ <i>k</i> ≤ 15, −21 ≤ <i>l</i> ≤ 24	−20 ≤ <i>h</i> ≤ 29, −22 ≤ <i>k</i> ≤ 22, −17 ≤ <i>l</i> ≤ 15	−28 ≤ <i>h</i> ≤ 17, −15 ≤ <i>k</i> ≤ 23, −17 ≤ <i>l</i> ≤ 13
reflexions collected	20754	24884	45596	19982	16068
reflexions unique	9394	13183	17010	10037	10527
refinement method	[<i>R</i> _{int} = 0.0687] full-matrix least-squares on <i>F</i> ²	[<i>R</i> _{int} = 0.0393] full-matrix least-squares on <i>F</i> ²	[<i>R</i> _{int} = 0.1255] full-matrix least-squares on <i>F</i> ²	[<i>R</i> _{int} = 0.0521] full-matrix least-squares on <i>F</i> ²	[<i>R</i> _{int} = 0.0367] full-matrix least-squares on <i>F</i> ²
data/restraints/parameters	9394/0/487	13183/0/379	17010/12/1039	10037/1/892	10527/1/892
absorption correction	Empirical	Empirical	Empirical	Empirical	Empirical
goodness-of-fit on <i>F</i> ² (GOF)	0.751	0.855	0.669	0.783	0.819
final <i>R</i> indices [<i>I</i> > 2 σ (<i>I</i>)]	<i>R</i> ₁ = 0.0448, <i>wR</i> ₂ = 0.0528	<i>R</i> ₁ = 0.0438, <i>wR</i> ₂ = 0.0854	<i>R</i> ₁ = 0.0443, <i>wR</i> ₂ = 0.0481	<i>R</i> ₁ = 0.0425, <i>wR</i> ₂ = 0.0633	<i>R</i> ₁ = 0.0435, <i>wR</i> ₂ = 0.0699
<i>R</i> indices (all data)	<i>R</i> ₁ = 0.1236, <i>wR</i> ₂ = 0.0690	<i>R</i> ₁ = 0.0921, <i>wR</i> ₂ = 0.0975	<i>R</i> ₁ = 0.1272, <i>wR</i> ₂ = 0.0565	<i>R</i> ₁ = 0.0712, <i>wR</i> ₂ = 0.0693	<i>R</i> ₁ = 0.0718, <i>wR</i> ₂ = 0.0758
largest difference peak and hole (e Å ⁻³)	0.436 and −0.610	1.497 and −0.858	0.710 and −0.949	0.897 and −0.571	1.001 and −0.410

$$^a R_1 = \sum ||F_{\text{obs}}| - |F_{\text{cal}}|| / \sum |F_{\text{obs}}|^{1/2}; wR_2 = [\sum w(F_{\text{obs}}^2 - F_{\text{cal}}^2)^2 / \sum w(F_{\text{obs}}^2)^2]^{1/2}; \text{GOF} = \{\sum [w(F_{\text{obs}}^2 - F_{\text{cal}}^2)^2] / (N_{\text{obs}} - N_{\text{par}})\}^{1/2}.$$

Obviously, a homoleptic complex or cluster [Ru_{*a*}(GaCp*)_{*b*}] is not accessible from a phosphine containing precursor. Thus, the all-hydrocarbon coordinated transition metal complex [Ru(η^2, η^2 -COD)(η^6 -COT)] (COD = 1,5-cyclooctadiene, C₈H₁₂, COT = 1,3,5-cyclooctatriene, C₈H₁₀) was chosen as an appropriate, phosphine-free precursor. As previously reported, the reaction of [Ru(η^2, η^2 -COD)(η^6 -COT)] with excess of GaCp* in toluene leads to the adduct [Ru(η^2, η^2 -COD)(η^4 -COT)(GaCp*)] rather than substitution products.²⁰ However, reaction of [Ru(η^2, η^2 -COD)(η^6 -COT)] with 3 molar equiv of GaCp* under hydrogen atmosphere leads to the substitution product [Ru(η^2, η^2 -COD)(GaCp*)₃] (**3**), under hydrogenation of the cyclooctatriene ligand (Scheme 1). It should be noted, that performing this reaction with excess of GaCp* under somewhat rougher conditions (110 °C, several hours) leads to full substitution of the olefinic ligands and formation of the dimeric, gallium bridged ruthenium-hydride [(μ -Ga)Ru₂H₃(GaCp*)₇] which has been previously communicated by us.³² Single crystals of **3**, suitable for X-ray diffraction studies, were obtained by slowly cooling a saturated hexane solution of **3** down to −30 °C for several days. Important crystallographic data are compiled in Table 1 and the molecular structure in the solid state is shown in Figure 2.

Compound **3** crystallizes in the triclinic space group *P* $\bar{1}$. The solid state structure reveals a distorted trigonal-bipyramidal ligand environment (Figure 3, see Table 1) in which two GaCp* ligands and one olefinic bond of the COD

ligand occupy the equatorial positions (Ga(2)–Ru–C(5) C(6)_{Centr.} *cis*-angle of 112.1°, C(5)C(6)_{Centr.}–Ru–Ga(3) *cis*-angle of 152.2°), while the remaining ligands are located in the axial positions (Ga(1)–Ru–C(1)C(2)_{Centr.} *trans*-angle of 160.6°). The Ru–Ga bond distances range from 2.364(1) Å for Ru–Ga(1) to 2.394(1) Å for Ru–Ga(2) with an average value of 2.375 Å and are therefore well in line with **1**. The Cp* groups of each low valent group 13 ligand are in a clear η^5 binding mode with Ga–Cp*_{centr.} bond lengths of 1.987–2.026 Å (average 2.002 Å). It should be noted that each Cp* group bound to the respective Ga atom is slightly bent out of the ideal position resulting in angles Ru–Ga(1)–Cp*_{centr.} of 159.9°, Ru–Ga(2)–Cp*_{centr.} of 161.8° and Ru–Ga(3)–Cp*_{centr.} of 165.1°, respectively. The COD ligand is characterized by a typical η^2, η^2 coordination mode with C–C and Ru–C bond distances similar to those of reported [Ru(η^2, η^2 -COD)_{*x*}(L)_{*y*}] complexes.^{22,33}

The ¹H NMR spectrum of **3** in C₆D₆ is in good agreement with the proposed structure of **3**, featuring two signals at δ = 3.90 ppm (s, 4H, C–H) and δ = 2.17 ppm (s, 8 H, CH₂) for the COD ligand and one signal at δ = 1.96 ppm (s, 45H, C₅Me₅) for the GaCp* ligands. The ¹³C spectrum does not bear any unusual features.

The reaction of [{Rh(η^2, η^2 -NBD)(PCy₃)₂}{BAR^F}] (NBD = norbornadiene, C₇H₈; Cy = cyclohexyl, -C₆H₁₁; {BAR^F} = B{[C₆H₃(CF₃)₂]₄} with 2 equiv of GaCp* in fluorobenzene at 80 °C gives a bright-red solution. After removal

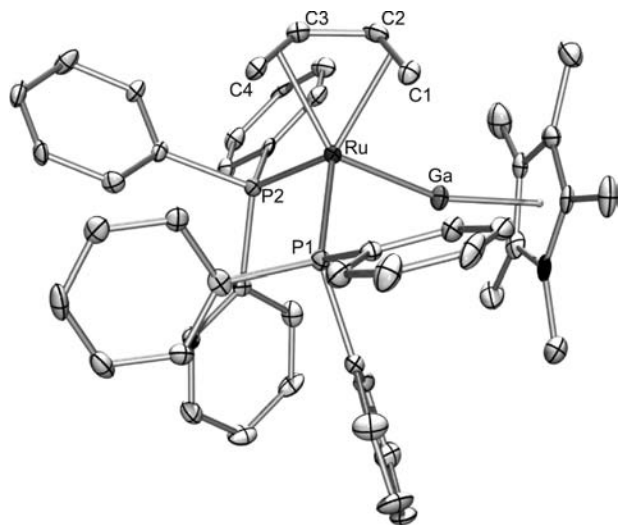


Figure 1. Molecular structure of **1** in the solid state as determined by single crystal X-ray crystallography (thermal ellipsoids are shown at the 50% probability level, hydrogen atoms have been omitted for clarity). Selected bond lengths (Å) and angles (deg): Ru–C(3) 2.154(4), Ru–C(4) 2.174(4), Ru–C(2) 2.185(4), Ru–C(1) 2.202(4), Ru–P(2) 2.303(1), Ru–P(1) 2.305(2), Ru–Ga 2.401(1), Ga–Cp*_{centr.} 2.001, C(3)C(4)_{Centr.}–Ru–Ga 139.9, P(1)–Ru–C(3)C(4)_{Centr.} 116.7, P(2)–Ru–C(3)C(4)_{Centr.} 93.4, C(1)C(2)_{Centr.}–Ru–Ga 88.3, C(1)C(2)_{Centr.}–Ru–P(1) 118.4, C(1)C(2)_{Centr.}–Ru–P(2) 137.2, Ru–Ga–Cp*_{centr.} 160.6, P(2)–Ru–P(1) 102.9(1), P(2)–Ru–Ga 96.4(1), P(1)–Ru–Ga 98.8(1), C(3)–C(2)–C(1) 117.0(4), C(2)–C(3)–C(4) 116.7(4).

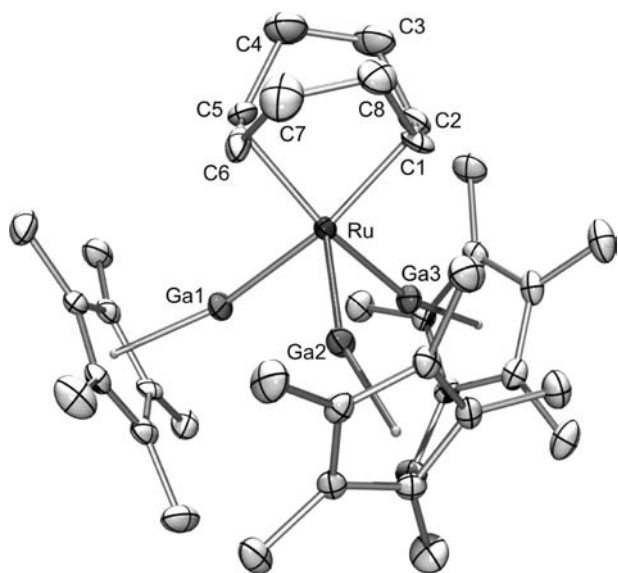


Figure 2. Molecular structure of **3** in the solid state as determined by single crystal X-ray crystallography (thermal ellipsoids are shown at the 50% probability level, hydrogen atoms have been omitted for clarity, carbon atoms are displayed in gray). Selected bond lengths (Å) and angles (deg): Ru(1)–C(6) 2.166(3), Ru(1)–C(5) 2.183(3), Ru–C(1) 2.189(3), Ru–C(2) 2.195(3), Ru–Ga(1) 2.364(1), Ru–Ga(3) 2.367(1), Ru–Ga(2) 2.394(1), Ga(1)–Cp*_{Centr.} 1.987, Ga(2)–Cp*_{Centr.} 2.026, Ga(3)–Cp*_{Centr.} 1.994, Ga(2)–Ru–C(5)C(6)_{Centr.} 112.1, C(5)C(6)_{Centr.}–Ru–Ga(3), C(5)C(6)_{Centr.}–Ru–Ga(1) 90.0, C(5)C(6)_{Centr.}–Ru–C(1)C(2)_{Centr.} 84.8, Ga(1)–Ru–C(1)C(2)_{Centr.} 160.6, Ga(2)–Ru–C(1)C(2)_{Centr.} 106.5, Ga(3)–Ru–C(1)C(2)_{Centr.} 91.8, Ga(1)–Ru–Ga(3) 84.1(1), Ga(1)–Ru–Ga(2) 92.7(1), Ga(3)–Ru–Ga(2) 95.4(1), Ru–Ga(1)–Cp*_{Centr.} 159.9, Ru–Ga(2)–Cp*_{Centr.} 161.8, Ru–Ga(3)–Cp*_{Centr.} 165.1.

of the solvent in vacuo and recrystallization of the residue by slow diffusion of *n*-hexane into a fluorobenzene solution at room temperature gives air-sensitive red crystals of $[\{\text{Rh}(\eta^2, \eta^2\text{-NBD})(\text{PCy}_3)(\text{GaCp}^*)_2\}\{\text{BAR}^{\text{F}}\}]$ (**4**) in yields around 80%

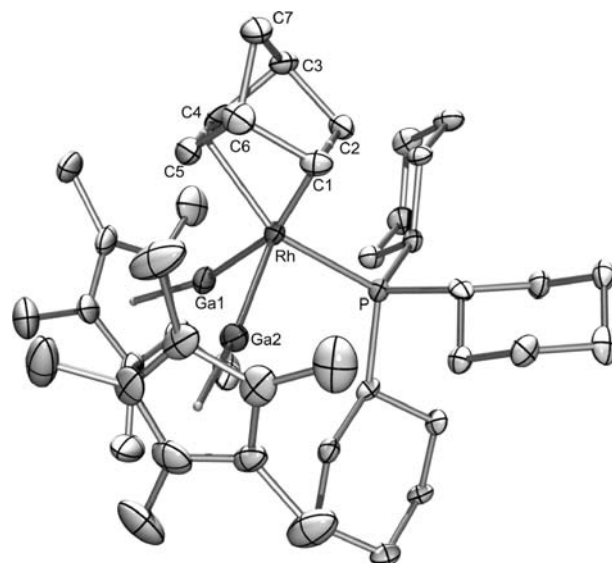


Figure 3. Molecular structure of the cationic part of **4** in the solid state as determined by X-ray single crystal diffraction (thermal ellipsoids are shown at the 30% probability level, hydrogen atoms have been omitted for clarity). Selected bond lengths (Å) and angles (deg): Rh–C(1) 2.184(4), Rh–C(2) 2.191(3), Rh–C(4) 2.210(3), Rh–C(5) 2.220(3), Rh–P(1) 2.337(1), Rh–Ga(1) 2.375(1), Rh–Ga(2) 2.441(1), Ga(1)–Cp*_{Centr.} 1.916, Ga(2)–Cp*_{Centr.} 1.983, Rh–Ga(1)–Cp*_{Centr.} 165.8, Rh–Ga(1)–Cp*_{Centr.} 166.3, P(1)–Rh–Ga(1) 89.6(0), P(1)–Rh–Ga(2) 102.3(1), Ga(1)–Rh–Ga(2) 96.4(1), C(1)C(2)_{Centr.}–Rh–Ga(1) 156.2, C(1)C(2)_{Centr.}–Rh–Ga(2) 103.6, C(1)C(2)_{Centr.}–Rh–P(1) 98.6, C(1)C(2)_{Centr.}–Rh–C(4)C(5)_{Centr.} 68.4, C(4)C(5)_{Centr.}–Rh–Ga(1) 94.2, C(4)C(5)_{Centr.}–Rh–Ga(2) 104.9, C(4)C(5)_{Centr.}–Rh–P(1) 152.0

(Scheme 2). It should be noted that use of one or 3 molar equiv of GaCp* in this reaction leads to the identical product **4**. The solid-state structure of **4** has been determined by a single crystal X-ray diffraction experiment. A POVray plot of **4** is shown in Figure 3, and important crystallographic data are summarized in Table 1. Compound **4** crystallizes in the monoclinic space group $P2(1)/n$. The rhodium atom is coordinated in a distorted trigonal bipyramidal environment by one GaCp* ligand and one double bond of the η^4 -NBD ligand in the axial positions, while the remaining GaCp* and the remaining NBD-double bond, as well as the tricyclohexylphosphine ligand, are located in the equatorial plane. The C(1)C(2)_{Centr.} ligand is found to be slightly bent toward the equatorial plane resulting in a Ga(1)–Rh–C(1)C(2)_{Centr.} angle of 156.2°. However, the ligands in the equatorial plane are found in positions which also deviate from the ideal trigonal bipyramidal structure resulting in angles of Ga(2)–Rh–C(3)C(4)_{Centr.} 104.9°, P(1)–Rh–C(3)C(4)_{Centr.} 152.0°, and Ga(2)–Rh–P(1) 102.3(1)°, respectively. The axial Rh–Ga bond distance is 2.375(1) Å, while the equatorial Rh–Ga bond length is slightly elongated with 2.441(1) Å, which is comparable to the Rh–GaCp* bond lengths in the reported salt $[\{\text{Rh}(\text{GaCp}^*)_4(\text{GaMe})\}\{\text{BAR}^{\text{F}}\}]$.¹⁷ Each Cp* group is η^5 -bound to the Ga atoms with an average Ga–Cp*_{centr.} bond length of 1.950 Å. The NBD ligand is characterized by a typical η^4 coordination mode with C–C and Rh–C bond distances similar to those of reported $[\text{Rh}(\eta^2, \eta^2\text{-NBD})_x(\text{L})_y]$ complexes.^{34–36}

The ¹H, ³¹P, and ¹³C NMR data are in good agreement with the solid state structure and do not bear any unusual features. In analogy to the synthesis of **3** starting from $[\text{Ru}(\eta^2, \eta^2\text{-COD})(\eta^6\text{-COT})]$, we treated a freshly prepared sample of the isolobal complex $[\{\text{Rh}(\eta^2, \eta^2\text{-COD})_2\}\{\text{BAR}^{\text{F}}\}]$

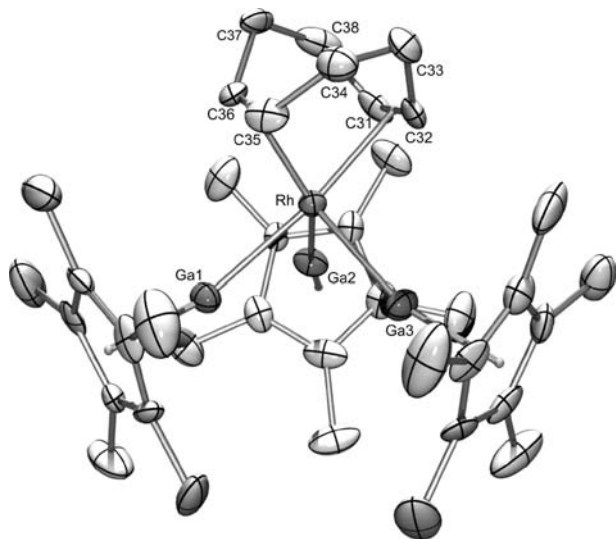
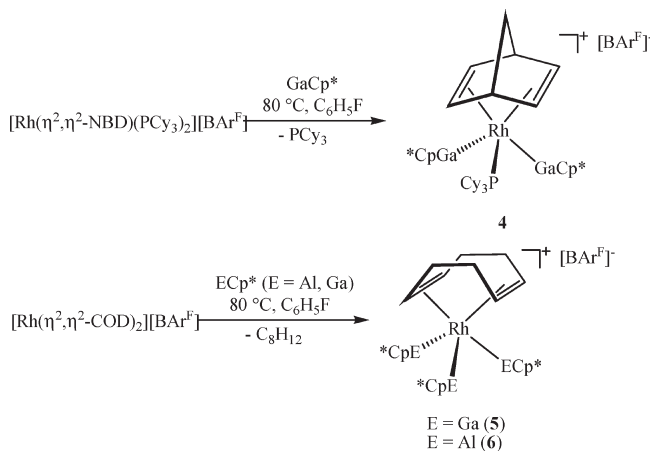


Figure 4. Molecular structure of the cationic part of **3** in the solid state as determined by X-ray single crystal diffraction (thermal ellipsoids are shown at the 50% probability level, hydrogen atoms have been omitted for clarity). Selected bond lengths (Å) and angles (deg): Rh–C(35) 2.181(6), Rh–C(36) 2.196(7), Rh–C(31) 2.216(7), Rh–C(32) 2.226(6), Rh–Ga(1) 2.359(1), Rh–Ga(2) 2.373(11), Rh–Ga(3) 2.405(1), Ga(1)–Cp*_{Centr.} 1.912, Ga(2)–Cp*_{Centr.} 1.933, Ga(3)–Cp*_{Centr.} 1.960, Rh–Ga(1)–Cp*_{Centr.} 161.2, Rh–Ga(1)–Cp*_{Centr.} 168.3, Rh–Ga(3)–Cp*_{Centr.} 163.4, Ga(1)–Rh–Ga(2) 84.7(1), Ga(1)–Rh–Ga(3) 88.1(1), Ga(2)–Rh–Ga(3) 98.7(1), C(31)C(32)_{Centr.}–Rh–Ga(1) 172.3, C(31)C(32)_{Centr.}–Rh–Ga(2) 95.4, C(31)C(32)_{Centr.}–Rh–Ga(3) 99.5, C(31)C(32)_{Centr.}–Rh–C(35)C(36)_{Centr.} 84.7, C(35)C(36)_{Centr.}–Rh–Ga(1) 89.8, C(35)C(36)_{Centr.}–Rh–Ga(2) 135.8, C(35)C(36)_{Centr.}–Rh–Ga(3) 124.9.

Scheme 2. Syntheses of the Rhodium Complexes **4**, **5**, and **6**



with 3 molar equiv of GaCp* in fluorobenzene at 80 °C. Subsequent crystallization by means of slow diffusion of *n*-hexane into this solution at 25 °C afforded air sensitive red crystals of $[\{\text{Rh}(\eta^2, \eta^2\text{-COD})(\text{GaCp}^*)_3\}\{\text{BAR}^{\text{F}}\}]$ (**5**) in a preparative yield of $\geq 80\%$ (Scheme 2). Notably, under identical conditions the reaction of $[\{\text{Rh}(\eta^2, \eta^2\text{-COD})_2\}\{\text{BAR}^{\text{F}}\}]$ with the low valent group 13 homologue AlCp* leads to the analogue complex $[\{\text{Rh}(\eta^2, \eta^2\text{-COD})(\text{AlCp}^*)_3\}\{\text{BAR}^{\text{F}}\}]$ (**6**) (see Scheme 2 and Supporting Information).

The solid state structure of **5** reveals a distorted trigonal bipyramidal environment for the rhodium center (Figure 4). The equatorial positions are occupied by two GaCp* ligands and one double bond of the COD ligand (Ga(3)–Rh–C(35)C(36)_{Centr.} *cis*-angle of 124.9°, C(35)C(36)_{Centr.}–Rh–Ga(2)

cis-angle of 135.8°) and the axial positions are occupied by the remaining GaCp* ligand and the second double bond of the COD ligand (Ga(1)–Rh–C(31)C(32)_{Centr.} *trans*-angle of 172.3°). The Rh–Ga bond distances range from 2.360(1) Å for Rh–Ga(1) to 2.405(1) Å for Rh–Ga(3) with an average value of 2.379 Å which is comparable to those in **4** and to previously reported Rh–GaCp* complexes.^{16,17,37,38} The Cp* groups of each low valent group 13 ligand are in a clear η^5 binding mode with Ga–Cp*_{centr.} bond lengths of 1.912–1.960 Å (average 1.935 Å). This distinct shortening of the Ga–Cp*_{centr.} distance in comparison to **3** is rationalized by the overall positive charge of the complex, leading to an increase in the ionic character of the Ga–Cp* bond. Each Cp* group is slightly bent, resulting in angles Rh–Ga(1)–Cp*_{centr.} of 161.2°, Rh–Ga(2)–Cp*_{centr.} of 168.3°, and Rh–Ga(3)–Cp*_{centr.} of 163.8°, respectively. The COD ligand is characterized by a typical η^2 - η^2 coordination mode with C–C and Rh–C bond distances similar to those of other $[\text{Rh}(\eta^4\text{-COD})_x(\text{L})_y]$ complexes. The ¹H spectrum of **3** in *d*⁸-thf is in good agreement with its solid state structure, with two signals at $\delta = 4.52$ ppm (s, 4H, C–H) and $\delta = 2.14$ ppm (s, 8 H, CH₂) for the COD ligand and one signal at $\delta = 2.06$ ppm (s, 45H, C₅Me₅) for the GaCp* ligands. The ¹³C spectrum does not bear any unusual features.

Conclusions

The reaction of olefin containing *d*⁸ metal complexes with GaCp* and AlCp* indeed leads to substitution of olefins by ECp* ligands. However, the very nature of the metal centers Ru⁰ and Rh^I as strong metal bases inhibits full substitution and thus allows the synthesis of ECp* complexes bearing olefins as co-ligands. The increased π -backbonding upon coordination of GaCp* is reflected by the C–C bond lengths of the coordinated olefins in the crystal structures of the products, for example, the butadiene complex **1** best described as a metallacyclopentene structure rather than a simple π -complex. As expected, full substitution of phosphines by ECp* is also not favored, which is attributable to the similar bonding energies of these ligands.

This class of compounds might be potentially used for the synthesis of higher nuclearity mixed metal clusters, considering that olefin ligands can be split off by hydrogenation from the transition metal in the presence of ECp* ligands, and even Cp* can be split off from coordinated group-13 center under proper conditions.³² Accordingly, these complexes should provide convenient building blocks for the synthesis of mixed metal clusters with M/Ga/Zn metal cores, since the ratio of M/Ga is reduced with respect to that of the homoleptic clusters. Moreover, the olefin ligands should serve at the same time as “protective groups” for later transformations such as substitution by E^IR or Zn^IR ligands, thus offering an intelligent synthetic access to mixed metal cluster growth reactions.

Experimental Section

General Remarks. All manipulations were carried out in an atmosphere of purified argon using standard Schlenk and glovebox techniques. Hexane, Toluene, THF, and Et₂O were dried using an mBraun Solvent Purification System; all other solvents were dried by distillation over standard drying agents. The final H₂O content in all solvents used was checked by Karl Fischer-Titration and did not exceed 5 ppm. $[\text{Ru}(\eta^4\text{-butadiene})(\text{PPh}_3)_3]$,^{39,40} $[\text{Ru}(\text{styrene})_2(\text{PPh}_3)_2]$,⁴¹ $[\text{Ru}(\eta^2, \eta^2\text{-COD})(\eta^6\text{-COT})]$,⁴²

$[\{\text{Rh}(\eta^2, \eta^2\text{-NBD})(\text{PCy}_3)_2\}\{\text{BAR}^{\text{F}}\}]$,^{43,44} $[\{\text{Rh}(\eta^2, \eta^2\text{-COD})_2\}\{\text{BAR}^{\text{F}}\}]$,⁴⁵ GaCp^* ,^{46,47} and AlCp^* ^{48–50} were prepared according to literature methods. Elemental analyses were performed by the Microanalytical Laboratory of the University of Essen. NMR spectra were recorded on a Bruker Avance DPX-250 spectrometer (^1H , 250.1 MHz; ^{13}C , 62.9 MHz) in at 298 K unless otherwise stated. Chemical shifts are given relative to TMS and were referenced to the solvent resonances as internal standards. The crystal structures were measured on a Oxford Excalibur 2 diffractometer using $\text{MoK}\alpha$ radiation ($\lambda = 0.71073 \text{ \AA}$). The structures were solved by direct methods using SHELXS-97 and refined against F^2 on all data by full-matrix least-squares with SHELXL-97 (SHELX-97 program package, Sheldrick, Universität Göttingen 1997).^{51,52}

Syntheses. **[Ru(η^4 -but)(PPh₃)₂(GaCp*)] (1).** To a solution of $[\text{Ru}(\eta^4\text{-but})(\text{PPh}_3)_3]$ (0.200 g, 0.212 mmol) in toluene (6 mL) was added GaCp^* (0.052 g, 0.254 mmol). The reaction mixture was stirred for 1 h at 80 °C, the solvent was removed in vacuo, and the residue was washed with a small amount of cold hexane (3 × 1 mL). The white solid was redissolved in a small amount of *n*-hexane, and the solution was cooled at –30 °C for 12 h. Colorless crystals were isolated by means of cannulation and dried in vacuo. Yield: 0.137 g (73%). Anal. Calcd for $\text{C}_{50}\text{H}_{51}\text{GaP}_2\text{Ru}$: C, 67.88; H, 5.81. Found: C, 66.98; H, 5.04. ^1H NMR $\delta_{\text{H}}(\text{C}_6\text{D}_6)$, 7.85–6.95 (m, 30H, PPh₃), 4.98 (br, 2H, syn 1,4-CH₂), 1.81 (s, 15H, GaCp*), 1.51 (br, 2H, CH), –0.66 (br, 2H, anti 1,4-CH₂). $^{13}\text{C}\{^1\text{H}\}$ NMR $\delta_{\text{C}\{\text{H}\}}(\text{C}_6\text{D}_6)$, 143.9 (d, $J = 30.5$ Hz), 134.0 (d, $J = 11.5$ Hz), 127.7 (d, $J = 27.4$ Hz), 114.0 (C_5Me_5), 75.1 (s, CH = CH₂), 36.5 (s, CH = CH₂) 10.1 (C_5Me_5). $^{31}\text{P}\{^1\text{H}\}$ NMR $\delta_{\text{P}}(\text{C}_6\text{D}_6) = 58.9$ (PPh₃).

[Ru(PPh₃)₂(GaCp*)₃] (2). To a solution of a freshly prepared sample of $[\text{Ru}(\eta^2\text{-C}_8\text{H}_8)_2(\text{PPh}_3)_2]$ (0.300 g, 0.360 mmol) in hexane (6 mL) was slowly added GaCp^* (0.236 g, 1.151 mmol) at –30 °C. The reaction mixture was slowly warmed to room temperature and stirred for further 30 min at 60 °C. After removal of all volatiles in vacuo the red residue was redissolved in *n*-hexane and slowly cooled to –30 °C while **2** crystallized in form of red needles. Yield: 0.300 g (67%). Anal. Calcd for $\text{C}_{66}\text{H}_{75}\text{Ga}_3\text{P}_2\text{Ru}$: C, 63.90; H, 6.09. Found: C, 63.11; H, 5.70. ^1H NMR $\delta_{\text{H}}(\text{C}_6\text{D}_6)$ 8.06–7.00 (m, 30H, PPh₃), 1.67 (s, 45H, GaCp*). $^{13}\text{C}\{^1\text{H}\}$ NMR $\delta_{\text{C}\{\text{H}\}}(\text{C}_6\text{D}_6)$, = 139.8 (d, $J = 29.4$ Hz), 135.0 (d, $J = 10.7$ Hz), 129.7 (d, $J = 2.4$ Hz), 114.5 (C_5Me_5), 11.2 (C_5Me_5). $^{31}\text{P}\{^1\text{H}\}$ NMR $\delta_{\text{P}}(\text{d}^8\text{-thf}) = 63.6$ (s, PPh₃).

[Ru(η^4 -COD)(GaCp*)₃] (3). A freshly prepared sample of $\text{Ru}(\text{C}_8\text{H}_{12})(\text{C}_8\text{H}_{10})$ (0.300 g, 0.951 mmol) was introduced into a Fischer–Porter bottle and then dissolved in hexane (5 mL). After addition of GaCp^* (0.625 g, 3.048 mmol) the reaction mixture was pressurized to 3 bar dihydrogen and stirred for 1 h at room temperature whereupon the solution turned red. The reaction mixture was transferred into a Schlenk tube, and all volatiles were removed in vacuo. The red solid was redissolved in a small amount of *n*-hexane, and the solution was cooled at –30 °C for 12 h. Pale red crystals were isolated by means of cannulation, washed with a small amount of cold *n*-hexane, and dried in vacuo. Yield: 0.651 g (83%). Anal. Calcd for $\text{C}_{38}\text{H}_{57}\text{Ga}_3\text{Ru}$: C, 55.38; H, 6.97. Found: C, 55.52; H, 7.62. ^1H NMR $\delta_{\text{H}}(\text{C}_6\text{D}_6)$ 3.90 (s, 4H, COD), 2.17 (s, 8H, COD), 1.96

(s, 45H, GaCp*). $^{13}\text{C}\{^1\text{H}\}$ NMR $\delta_{\text{C}\{\text{H}\}}(\text{C}_6\text{D}_6)$ 113.5 (C_5Me_5), 45.4 (CH, COD), 34.9 (s, CH₂, COD), 10.3 ppm (C_5Me_5).

[[Rh(η^2, η^2 -NBD)(PCy₃)₂](GaCp*)₂][BAR^F] (4). To a solution of $[\{\text{Rh}(\text{PCy}_3)_2(\eta^4\text{-NBD})\}\{\text{BAR}^{\text{F}}\}]$ (0.280 g, 0.173 mmol) in fluorobenzene (6 mL) was added GaCp^* (0.078 g, 0.380 mmol). The reaction mixture was stirred for 1 h at 80 °C. The solvent was removed in vacuo, and the residue was washed with hexane (3 × 4 mL). Single crystals can be obtained by slow diffusion of hexane into a fluorobenzene solution. Yield: 0.239 g (79%). Anal. Calcd for $\text{C}_{77}\text{H}_{83}\text{BF}_{24}\text{Ga}_2\text{PRu}$: C, 52.89; H, 4.78. Found: C, 51.98; H, 4.19. ^1H NMR $\delta_{\text{H}}(\text{d}^8\text{-thf})$ 7.79 (s, 8 H, BAR^F), 7.58 (s, 4H, BAR^F), 3.64 (br s, 4H, NBD), 3.35 (br s, 2H, NBD), 2.10 (s, 30H, GaCp*), 1.63 (s, 33H, PCy₃). $^{13}\text{C}\{^1\text{H}\}$ NMR $\delta_{\text{C}\{\text{H}\}}(\text{d}^8\text{-thf})$ 163.0 (q, $J = 49.7$ Hz, [BAR^F]), 135.8 ([BAR^F]), 130.2 (q, $J = 31.7$ Hz, [BAR^F]), 125.7 (q, $J = 272.2$ Hz, [BAR^F]), 118.4 ([BAR^F]), 115.9 (C_5Me_5), 62.1 (s), 48.0 (s), 36.7 (t, $J = 6.0$ Hz), 32.7 (br), 27.7 (q, $J = 59.8$ Hz), 10.4 (C_5Me_5). $^{31}\text{P}\{^1\text{H}\}$ NMR $\delta_{\text{P}}(\text{d}^8\text{-thf}) = 62.0$ (d, $J = 124.1$ Hz, PCy₃).

[[Rh(η^2, η^2 -COD)(GaCp*)₃][BAR^F] (5). To a solution of $[\{\text{Rh}(\text{cod})_2\}\{\text{BAR}^{\text{F}}\}]$ (0.300 g, 0.254 mmol) in fluorobenzene (6 mL) was added GaCp^* (0.172 g, 0.839 mmol). The reaction mixture was stirred for 1 h at room temperature. The solvent was removed in vacuo, and the residue was washed with hexane (3 × 4 mL). Single crystals can be obtained by slow diffusion of hexane into a fluorobenzene solution. Yield: 0.378 g (88%). Anal. Calcd for $\text{C}_{70}\text{H}_{69}\text{BF}_{24}\text{Ga}_3\text{Rh}$: C, 49.77; H, 4.12. Found: C, 50.12; H, 4.41. ^1H NMR $\delta_{\text{H}}(\text{d}^8\text{-thf})$ 7.79 (s, 8 H, BAR^F), 7.58 (s, 4H, BAR^F), 4.52 (s, 4H, COD), 2.14 (s, 8H, COD), 2.06 (s, 45H, GaCp*). $^{13}\text{C}\{^1\text{H}\}$ NMR $\delta_{\text{C}\{\text{H}\}}(\text{d}^8\text{-thf})$ 162.8 (q, $J = 49.6$ Hz, [BAR^F]), 135.6 ([BAR^F]), 130.0 (q, $J = 31.7$ Hz, [BAR^F]), 125.5 (q, $J = 272.3$ Hz, [BAR^F]), 118.2 ([BAR^F]) 115.7 (C_5Me_5), 66.1 (d, $J = 8.7$ Hz, CH, COD), 33.9 (s, CH₂, COD), 10.0 ppm (C_5Me_5).

[[Rh(η^2, η^2 -COD)(AlCp*)₃][BAR^F] (6). After a Schlenk tube was charged with a pure crystalline sample of $[\{\text{Rh}(\text{cod})_2\}\{\text{BAR}^{\text{F}}\}]$ (0.300 g, 0.254 mmol) and AlCp^* (0.124 g, 0.762 mmol), fluorobenzene (6 mL) was added. After the reaction mixture was stirred for 1 h at 80 °C the solvent was removed in vacuo, and the residue was washed with hexane (3 × 4 mL). Single crystals can be obtained by slow diffusion of Et₂O into a THF solution. Yield: 0.248 g (63%). Anal. Calcd for $\text{C}_{70}\text{H}_{69}\text{BF}_{24}\text{Al}_3\text{Rh}$: C, 53.86; H, 4.46. Found: C, 54.66; H, 4.48. ^1H NMR $\delta_{\text{H}}(\text{CD}_2\text{Cl}_2)$ 7.75 (s, 8 H, BAR^F), 7.58 (s, 4H, BAR^F), 4.17 (s, 4H, COD), 2.15 (s, 8H, COD), 2.02 (s, 45H, GaCp*). $^{13}\text{C}\{^1\text{H}\}$ NMR $\delta_{\text{C}\{\text{H}\}}(\text{CD}_2\text{Cl}_2)$ 162.3 (q, $J = 49.7$ Hz, [BAR^F]), 135.4 ([BAR^F]), 129.4 (q, $J = 31.4$ Hz, [BAR^F]), 125.2 (q, $J = 272.4$ Hz, [BAR^F]), 118.0 ([BAR^F]) 116.0 (C_5Me_5), 63.1 (d, $J = 6.8$ Hz, CH, COD), 34.6 (s, CH₂, COD), 10.6 ppm (C_5Me_5).

Acknowledgment. T.C. is grateful for a fellowship from the Fonds der Chemischen Industrie and for support by the Ruhr University Research School.

Supporting Information Available: Additional information as noted in the text. This material is available free of charge via the Internet at <http://pubs.acs.org>.